

Late Quaternary temperature variability described as abrupt transitions on a $1/f$ noise background

Martin Rypdal¹ and Kristoffer Rypdal¹

¹Department of Mathematics and Statistics, University of Tromsø The Arctic University of Norway, Tromsø, Norway

Correspondence to: Martin Rypdal (martin.rypdal@uit.no)

Abstract. In order to have a scaling description of the climate system that is not inherently non-stationary, the rapid shifts between stadials and interstadials during the last glaciation (the Dansgaard-Oeschger events) cannot be included in the scaling law. The same is true for the shifts between the glacial and interglacial states in the quaternary climate. When these events are omitted from a scaling analysis the climate noise is consistent with a $1/f$ law on time scales from months to 10^5 years. If the records analysed include the shift events, the effect is to create a break the scaling from a $1/f$ law to a $1/f^\beta$ law, with $1 < \beta < 2$. No evidence of multifractal intermittency have been found in any of the temperature records investigated, and the events are not a natural consequence of multifractal scaling.

10 1 Introduction

The temporal variations in Earth's surface temperature are well described as *scaling* on an extended range of time scales. In this parsimonious characterisation, a parameter β describes how the fluctuation levels on the different time scales are related to each other. The β -parameter can be defined via the scaling of the spectral density function of the signal by the relation $S(f) \sim f^{-\beta}$. An alternative is to measure range of the variability on the longest time scales within a time window of length Δt by

$$T_{\Delta t}(t) = \left| \frac{2}{\Delta t} \sum_{i=t}^{t+\Delta t/2} T(t) - \frac{2}{\Delta t} \sum_{i=t+\Delta t/2}^{t+\Delta t} T(t) \right|,$$

and to define β via the following relation (Lovejoy and Schertzer, 2013):

$$\text{Var}[T_{\Delta t}(t)] \sim \Delta t^{\beta-1}. \tag{1}$$

20 In this description, the temperature fluctuations would decrease with scale if $\beta < 1$, implying that the climate fluctuations become less prominent as we consider longer time scales, a picture which is somewhat different than the rich long-range variability indicated by proxy reconstructions of past climate. On the other hand, a value $\beta > 0$ would imply that variability increases with scale, a property

that (if it were valid on a large range of time scales) would lead to levels of temperature variability
25 inconsistent with reality. It is therefore a natural *a priori* working hypothesis, that Earth’s typical
temperature fluctuations, the climate noise, is characterised by $\beta \simeq 1$. Such a process is called a $1/f$
noise.

The $1/f$ description of Earth’s temperature is of course an idealised model. The reality is that the
climate system consists of many components that respond to perturbations on different characteris-
30 tic time scales, and the temperature signal can be seen as an aggregation of signals with different
time-scale characteristics. Since it is difficult to recognise pronounced time scales in the tempera-
ture records, a scaling description is both convenient and accurate. However, we are aware that the
scaling is not perfect, and that there are structures in the climate system that deviate from the scaling
law. One example is the El Niño Southern Oscillation (ENSO), which places larger fluctuations on
35 the times scales of a few years than what can be expected from a scaling model. Other examples are
the Dansgaard-Oeschger (DO) cycles in the Greenland climate during the last glacial period, encom-
passing repeated and rapid shifts between a cold stadial state and a much warmer interstadial state.
The result of this phenomena is that the glacial climate on Greenland has much larger millennial-
scale fluctuations than what can be expected from a $1/f$ description. However, as we demonstrate in
40 this paper, the temperature variations of both the stadial and interstadial climate states fit well with
the $1/f$ -scaling, telling us that the deviation from $1/f$ scaling in the glacial climate arise from these
regime shifting events. As we go to even longer time scales, we also observe anomalous fluctuation
levels on time scales from 10^4 to 10^5 years that can be identified with the shifting between glacial
and interglacial conditions.

45 One could argue that the DO cycles and the glaciation cycles are intrinsic to the climate system
and should not be treated as special events, and their variations should be reflected in a scaling
description of the climate. For instance, Lovejoy (2014) *et al.* consider a “break” in the scaling law
with an exponent $\beta \approx 1.8$ on time scales longer than a century. A scaling model invoking two scaling
regimes can account for the millennial-scale temperature fluctuations that are produced by the DO
50 cycles, which are anomalous with respect to a $1/f$ model. However, the estimated scaling exponent
will depend on the average “density” of DO events in the ice-core record used for the estimate, and
since the events are not uniformly distributed over time, there is no uniquely defined scaling exponent
for the last glacial period. Moreover, the scaling law would not be useful as a climate-noise model
for determining the significance of particular trends and events, such as the anthropogenic warming
55 in the last century.

The main message of this paper is that the $1/f$ noise characterisation of the temporal fluctuations
in global mean surface temperature is very robust. It is an accurate description for the Holocene
climate, but it is also valid under both stadial and interstadial conditions during glaciations, and
during both glacial and interglacial conditions in the quaternary climate. The $1/f$ character of the
60 climate noise provides us with robust estimates of future natural climate variability, even in present

state of global warming. Such an estimate would of course be invalidated by a future regime shift (a tipping point) to a warmer climate state provoked by anthropogenic forcing. A future observed change in the $1/f$ character of the noise could therefore be taken as an early warning signal for such a shift.

65 2 Data, methods and results

The analysis in this work is based on four data sets for temperature fluctuations: the HadCRUT4 monthly global mean surface temperature (Morice et al., 2012) in the period 1880-2011 CE (Common Era), the Moberg Northern Hemisphere reconstruction for annual mean temperatures in the years 1-1978 CE (Moberg et al., 2005), as well as temperature reconstructions from the North Greenland Ice Core Project (NGRIP) (Andersen et al., 2004) and the European Project for Ice Coring in Antarctica (EPICA) (Augustin et al., 2004). For the NGRIP ice core we have used 20-yr means of $\delta^{18}\text{O}$ going back 60 kyr. For the EPICA ice core we have temperature reconstructions going back over 300 kyr, but the data is sampled at uneven time intervals and the time between subsequent data points becomes very large as we go back more than 200 kyr. In addition we have used annual data for radiative forcing in the time period 1880-2011 CE (Hansen, 2005) to remove the anthropogenic component in HadCRUT4 data. Plots of all four data records are shown in Fig. 1.

2.1 Global versus local scaling

On the face of it, it is difficult to discern scaling laws for the climate noise on time scales longer than millennia, since we do not have high-resolution global (or hemispheric) temperature reconstructions for time periods longer than two kyr. The ice core data available only allow us to reconstruct temperatures locally in Greenland and Antarctica, and we know from the instrumental record that local and regional continental temperatures scale differently from the global mean surface temperatures on time scales shorter than millennial. The differences we find are that local temperature scaling exponents β_l are smaller than global temperature exponents β_g , and that the ocean temperatures scale with higher exponents than land temperatures. Since there are strong spatial correlations in the climate system, it is possible that all local temperatures are scaling with a lower exponent than the global. In (Rypdal et al., 2015) this phenomenon is illustrated in an explicit stochastic spatio-temporal model. In this model, which is fitted to observational instrumental data, we find the relationship $\beta_g = 2\beta_l$. This relationship is derived under the highly inaccurate assumption that all local temperatures scale with the same exponent, but it is still a useful approximation in the following, where we will argue that we can use local and regional temperature records to discern the scaling of the global mean surface temperature on time scales of 10 kyr and longer. We do this by showing that the assumption that $\beta_g/\beta_l > 1$ is valid on very long times scales leads to the impossible result that the variance of

global averages become larger than the mean variance of local averages. Thus we conclude that β_l converges to β_g on sufficiently long time scale, and we estimate an upper limit on that time scale.

Let us denote by σ_g and σ_l the standard deviations of the global surface temperature and a local temperature respectively, on a monthly time scale. From Eq. (1) it follows that the ratio between the variances for the global and local temperatures at time scale Δt is

$$\rho = \left(\frac{\sigma_g}{\sigma_l}\right)^2 \left(\frac{\Delta t}{\tau}\right)^{\beta_g - \beta_l},$$

where $\tau = 1$ month. Unless we expect global temperatures to have larger variations than the local temperature at time scale Δt (the global temperature can not have a larger standard deviation than the average standard deviation of the local temperatures) we must have $\rho > 1$, or equivalently,

$$\Delta t < \tau \left(\frac{\sigma_l}{\sigma_g}\right)^{2/(\beta_g - \beta_l)}.$$

On the time scale of months, the fluctuation levels of continental temperatures is about two orders of magnitude larger than the fluctuation level for the global mean temperature. If we also use $\beta_g = 1$ and $\beta_l = 1/2$ we obtain the condition $\Delta t < 10^5$ months ~ 10 kyr, i.e., on time scales longer than 10 kyr the ratio β_g/β_l can no longer be larger than unity. A similar estimate can be obtained from the NGRIP ice core data. In the Holocene the 20-yr resolution temperature reconstructions from Greenland has a standard deviation which is about five times greater than the 20-yr moving average of the Moberg reconstruction for the Northern hemisphere. Applying the same argument restricts the time scale for which Greenland scaling exponent is smaller than the global scaling exponent to approximately 10 kyr.

Based on the reasoning above, we expect scaling of the ice core data to be similar to the global scaling on sufficiently long time scales. In the remainder of this paper we demonstrate that the scaling in the ice core data on time scales up to hundreds of kyr is similar to the $1/f$ scaling we observe in global temperature up to a few millennia. This suggests that the $1/f$ scaling on very long time scales in ice core data is a reflection of the scaling in global temperatures on these scales.

2.2 Methods for estimation of scaling

We use two methods to analyse the scaling of temperature records. The first is a simple periodogram estimation of the spectral power density $S(f)$. This estimator can also be applied to data with uneven time sampling using the Lomb-Scargle method (Lomb, 1976). The other method is to take the wavelet transform of the temperature data:

$$W(t, \Delta t) = \frac{1}{\sqrt{\Delta t}} \int T(t') \psi\left(\frac{t-t'}{\Delta t}\right) dt' \quad (2)$$

and construct the mean square of the wavelet coefficients. This is a standard technique for estimating the scaling exponent β (Malamud and Turcotte, 1999), and it is known that $\langle |W(t, \Delta t)|^2 \rangle \sim \Delta t^\beta$.

We choose to use the so-called Haar wavelet

$$\psi(t) = \begin{cases} 1 & t \in [0, 1/2) \\ -1 & t \in [1/2, 1) \\ 0 & \text{otherwise} \end{cases},$$

120 and the integral in Eq. 2 is computed as a sum. The method can be adapted to the case of unevenly sampled data using the method described in (Lovejoy, 2014). In this work, we obtain very similar results using the periodogram and the wavelet transform. These are methods for investigating the so-called second-order statistics of the data, which represents the information contained in the auto-covariance function. Claims have been made that higher-order statistics in the form of a multi-
125 fractal characterization is an essential part of the statistical description of these data (e.g., Lovejoy and Schertzer (2013), Chapter 11). For this reason we include a multifractal analysis of the data in Section 2.4.

2.3 Results of second-order analysis

In Fig. 2 we show the wavelet fluctuation $\langle |W(t, \Delta t)|^2 \rangle$ estimated for two different segments of the
130 NGRIP data. Both time series have the same number of data points and both represent time intervals of 8500 years. The differences between the two time series is that one contains DO cycles, whereas the other does not. The estimated wavelet fluctuations and the spectral density scale very differently for the two time series, and this motivates us to separate stadial and interstadial conditions when we analyse the scaling in NGRIP data. This separation is shown in Fig. 1(a), where the red curve
135 represents the $\delta^{18}\text{O}$ concentration in interstadial periods and the blue curve represents the $\delta^{18}\text{O}$ concentration in stadial periods. We have followed Svensson et al. (2008) in defining the dates for the onsets of the interstadials and we have defined the start dates for the stadial periods to be just after the rapid temperature decrease that typically follows the slow cooling in the interstadial periods. In Fig. 3 we show the spectral density function and the wavelet scaling function for the stadial data (red
140 diamonds) and the interstadial periods (purple triangles), which both display an approximate $1/f$ scaling, but where the fluctuation variance in the stadial data is larger than in the interstadial data. These results are different from what is obtained when considering the NGRIP data (during the last glaciation) as a single time series (shown as blue diamonds). If we were to define a single scaling exponent for the whole time series, then we would obtain an estimate $\beta \approx 1.4$.

145 Fig. 3 shows that the scaling of the stadial and interstadial NGRIP data are similar to the scaling of global temperatures on shorter time scales. We have included an analysis of the instrumental temperature record both with (green triangles) and without the anthropogenic component (green disks). The anthropogenic component can be removed by subtracting the response to the anthropogenic forcing in a simple linear response model of the type considered in (Rypdal and Rypdal, 2014). We have
150 also included an analysis of the Moberg Northern Hemisphere reconstruction (black squares), and

we observe that the composite scaling wavelet variance function and the composite spectral density function obtained by combining the instrumental data with the Moberg reconstruction, is consistent with a $1/f$ model on time scales from months to centuries. Since the NGRIP data also shows $1/f$ scaling, and since we believe that the scaling of the NGRIP data is a reflection of global scaling on time scales longer than a millennium, it is illustrative to adjust the fluctuation levels of the NGRIP data so that its Holocene part has a standard deviation close to that of the standard deviation of the 20-year means of the Moberg reconstruction in the same time period. This means that we use the adjusted NGRIP data as a proxy for global temperature on millennial scales. The effect of this adjustment is only a vertical shift of the wavelet scaling function and the spectral density functions in the double-logarithmic plots, so that it becomes easier to compare the scaling of the NGRIP data with the Moberg reconstruction and the instrumental data. We do not apply any adjustments of the fluctuation levels of the stadial and interstadial periods relative to each other. The same adjustment is applied to the EPICA data, and here we also consider the scaling of the glacial and interglacials separately as shown in Fig. 1(b). The scaling estimated from the EPICA data for glacial periods (black crosses in Fig. 3) follow the almost the same scaling as the NGRIP data analysed as a single time series (blue diamonds). This shows that the glacial climates have similar characteristics in Greenland and in Antarctica. Careful examination of the figure shows that the fluctuations grow slightly faster with the scale Δt in the NGRIP time series than for the glacial periods of the EPICA time series. This is expected since the regime shifting events in Antarctica (that are known to be connected with the DO cycles (WAIS Divide Project Members, 2015)) are much less pronounced than on Greenland. In the EPICA data we cannot estimate a scaling exponent for the dynamics in periods without regime shifts, but our results for the EPICA data are consistent with a description of the climate as a $1/f$ climate noise plus regime shifts. If we analyse the EPICA data without omitting the interglacials, then the fluctuations increase even faster with the scale Δt (orange stars in Fig. 3). This effect is completely analogous to the effect of shifting between the stadial and interstadial conditions during glaciations.

2.4 Results of multifractal analysis

The exponent β is well-defined as long as the power spectral density function $S(f)$ is a power law in f , or equivalently if the wavelet fluctuation function $E|W(t, \Delta t)|^2$ is a power law in Δt . If well-defined, the β exponent is related to the temporal correlations in the signal via simple formulas. In fact, for a (zero-mean) stationary process $T(t)$ with $-1 < \beta < 1$ we have $\langle T(t)T(t + \Delta t) \rangle \sim (\beta + 1)\beta\Delta t^{\beta-1}$ and for a (zero-mean) process with stationary increments and $1 < \beta < 3$ we have $\langle \Delta T(t)\Delta T(t + \Delta t) \rangle \sim (\beta - 1)(\beta - 2)\Delta t^{\beta-3}$, where $\Delta T(t)$ is the increment process of $T(t)$ (Rypdal and Rypdal, 2012). Thus, the results presented so far in this paper do not rely on any assumptions of self-similar or multifractal scaling. It is only assumed that the second-order fluctuation functions $\langle |W(t, \Delta t)|^2 \rangle$ are well approximated by power-laws over an extended range of time scales.

A more complete scaling analysis can be performed if one imposes the more restrictive assumption that the wavelet-based structure functions $\langle |W(t, \Delta t)|^q \rangle$ are power-laws in Δt , not only for $q = 2$, but for an interval of q -values. It is then it is possible to define a scaling function $\tau(q)$ via the relation

190 $\langle |W(t, \Delta t)|^q \rangle \sim \Delta t^{\tau(q)}.$

We observe that $\tau(2) = \beta$. If $T(t)$ is self-similar (or if $T(t)$ is the increment process of a self-similar process in the case $\beta < 1$) we have $\tau(q) = \beta q/2$, but in general, the $\tau(q)$ may be concave. Processes that exhibit power-law structure functions and strictly concave scaling functions can be characterized as multifractal intermittent.

195 If Fig. 4 we present a multifractal analysis of the data sets considered in this paper using q -values in the range from 0.1 to 4. For the Holocene we find linear scaling functions for both the instrumental record and the Moberg Northern Hemisphere reconstruction, and in the NGRIP data we find linear scaling functions for the both the stadial periods and the interstadial periods when these are analysed separately, although, as we have already seen, there is a deviation from the $1/f$ scaling in the stadial
 200 periods for time scales shorter than about 200 yrs. If the NGRIP record is analysed with both stadial and interstadial stages included, then it is not clear how to define the scaling function since the shifts between the two types of stages causes a “break” in the power-law scaling of the wavelet-based structure functions. If we define $\tau(q)$ using the time scales shorter than 2 kyr we obtain a linear scaling function corresponding to $\beta = 1.14$, and if we use the time scales longer than 4 kyr we obtain
 205 a linear scaling function corresponding to $\beta = 1.78$. In neither case do we obtain a strictly concave scaling function. A linear scaling function is also obtained if we disregard the “break” in the scaling and fit power laws using all the available time scales. In this case the scaling function corresponds to $\beta = 1.26$. For the periods of the EPICA record that corresponds to ice ages, we find wavelet-based structure functions that are closer to power-laws than what is observed in the NGRIP record. This
 210 is expected since the abrupt transitions between cold and warm periods is much less pronounced in Antarctica than in Greenland. The scaling function for the ice-age periods in the EPICA data is linear and corresponds to $\beta = 1.18$.

The results discussed above show that there is no evidence of multifractal intermittency in the temperature records analysed in this paper. This is not very surprising and could be established by
 215 direct inspection of the data record. The trained observer would use the fact that if $\tau(q)$ is strictly concave, then the kurtosis of $W(t, \Delta t)$,

$$\frac{\langle |W(t, \Delta t)|^4 \rangle}{\langle |W(t, \Delta t)|^2 \rangle^2} \sim \Delta t^{\tau(4) - 2\tau(2)},$$

is decreasing as a power-law function of Δt , and is therefore leptokurtic¹ on the shorter time scales Δt . Multifractal intermittency also implies that the amplitudes of the random fluctuations are clustered in time, on all time scales, as observed in intermittent turbulence or financial time series (see
 220

¹A distribution is leptokurtic if it has high kurtosis compared with a normal distribution. This means that the probability density function has a high central peak and fatter tails.

e.g., Bouchaud and Muzy (2003)). These are *not* prominent features in the time series analysed in paper. For the NGRIP data, the $\delta^{18}\text{O}$ ratio slightly deviates from a normal distribution as a result of the DO events, but this is not well described by a multifractal model since that would require the wavelet-based structure functions to be power-laws in Δt . In fact, what we show in this paper is that
225 effect of DO events is to break the scaling, rather than to produce multifractal scaling.

3 Discussion and concluding remarks

Accurate characterization of the climate noise is essential for the detection and evaluation of anthropogenic climate change. For instance, when we apply standard statistical methods for estimating the significance of a temperature trend, the result depends crucially on the so-called error model, i.e.,
230 the model for the climate noise. There is strong evidence that the temperature fluctuations are better described by scaling models than by so-called red-noise models (or AR(1)-type models). However, simply characterizing the climate noise as scaling does not specify an error model. The exponent in the scaling law (the β parameter) must also be determined, and it is usually determined from the same signal as we are testing for trends. Most estimators of β are sensitive to trends, providing too
235 large β -estimates when applied to signals with strong trends. So if we estimate β under the assumption that our null hypothesis (no trend) is true, then we are being led to a model with a value of β which is too large if the alternative hypothesis is true (there is a real trend). The large value of β will then lead us to believe that the climate noise can produce pseudo-trends comparable to the estimated trend in the signal, and the result is that we have a test with low statistical power (the probability of
240 detecting a significant trend is low even if there is a real trend). It is important to realize that there is nothing formally wrong with using a trend-detection test with low power. It only means that it will be difficult to make statistical significant conclusions about the observed trends. The lack of statistical significance under a weak test does not mean that the trends are not real. It would however be incorrect to give a general characterization of the climate noise by the exponent β if it is likely
245 that the β -estimate is strongly biased by the presence of a trend.

One approach to the problem described above is to apply some type of de-trending to the signal prior to the estimation of β . This may seem to be an inconsistent step, since the β should be estimated under the assumption that the null hypothesis is true. However, since de-trending only has a small effect if the null hypothesis is true, de-trending is valid under both the null hypothesis and the
250 alternative hypothesis. If de-trending is applied, the statistical powers of the standard trend-detection techniques for scaling processes are greatly improved.

Another approach, which is the motivation for this paper, is to characterize the scaling of the climate noise from pre-industrial temperature records. If we are to use the scaling exponent estimated from pre-industrial records to demonstrate the anomalous climate event associated anthropogenic
255 influence, we must be confident that the temperature scaling does not change significantly over

time. We must also be confident that the scaling is robust, in the sense that it is not too sensitive to moderate changes in the climate state. The main result of this paper is that unless the climate system experiences dramatic regime shifting events, we can be confident that the natural fluctuations in global surface temperature is approximated by $1/f$ -type scaling on a large range of time scales.

260 This result makes it easy to determine, on any time scale, if the observed increase in global mean surface temperature is inconsistent with the natural variability, and by how much.

Acknowledgements. This paper was supported by the the Norwegian Research Council (KLIMAFORSK programme) under grant no. 229754.

References

- 265 Andersen, K. K., Azuma, N., Barnola, J. M., Bigler, M., Biscaye, P., Caillon, N., Chappellaz, J., Clausen, H. B., Dahl-Jensen, D., Fischer, H., Flückiger, J., Fritzsche, D., Fujii, Y., Goto-Azuma, K., Grønbold, K., Gundestrup, N. S., Hansson, M., Huber, C., Hvidberg, C. S., Johnsen, S. J., Jonsell, U., Jouzel, J., Kipfstuhl, S., Landais, A., Leuenberger, M., Lorrain, R., Masson-Delmotte, V., Miller, H., Motoyama, H., Narita, H., Popp, T., Rasmussen, S. O., Raynaud, D., Röthlisberger, R., Ruth, U., Samyn, D., Schwander, J., Shoji, H.,
- 270 Siggard-Andersen, M. L., Steffensen, J. P., Stocker, T., Sveinbjörnsdóttir, A. E., Svensson, A., Takata, M., Tison, J. L., Thorsteinsson, T., Watanabe, O., Wilhelms, F., and White, J. W. C.: High-resolution record of Northern Hemisphere climate extending into the last interglacial period, *Nature*, 431, 147–151, 2004.
- Augustin, L., Barbante, C., Barnes, P. R. F., Marc Barnola, J., Bigler, M., Castellano, E., Cattani, O., Chappellaz, J., Dahl-Jensen, D., Delmonte, B., Dreyfus, G., Durand, G., Falourd, S., Fischer, H., Flückiger, J., Hansson, M. E., Huybrechts, P., Jugie, G., Johnsen, S. J., Jouzel, J., Kaufmann, P., Kipfstuhl, J., Lambert, F., Lipenkov, V. Y., Littot, G. C., Longinelli, A., Lorrain, R., Maggi, V., Masson-Delmotte, V., Miller, H., Mulvaney, R., Oerlemans, J., Oerter, H., Orombelli, G., Parrenin, F., Peel, D. A., Petit, J.-R., Raynaud, D., Ritz, C., Ruth, U., Schwander, J., Siegenthaler, U., Souchez, R., Stauffer, B., Peder Steffensen, J., Stenni, B., Stocker, T. F., Tabacco, I. E., Udisti, R., van de Wal, R. S. W., van den Broeke, M., Weiss, J., Wilhelms, F., Winther, J.-G.,
- 280 Wolff, E. W., and Zucchelli, M.: Eight glacial cycles from an Antarctic ice core, *Nature*, 429, 623–628, 2004.
- Bouchaud, J.-P. and Muzy, J.-F.: Financial Time Series: From Batchelier’s Random Walks to Multifractal Cascades, in *The Kolmogorov Legacy in Physics, Lecture Notes in Physics*, 636, 229–246, Springer-Verlag, Berlin Heidelberg, 2003.
- Hansen, J.: Earth’s Energy Imbalance: Confirmation and Implications, *Science*, 308, 1431–1435, 2005.
- 285 Lomb, N. R.: Least-squares frequency analysis of unequally spaced data, *Astrophys Space Sci*, 39, 447–462, 1976.
- Lovejoy, S. and Schertzer, D.: *The Weather and Climate: Emergent Laws and Multifractal Cascades*, Cambridge University Press, New York, NY, 2013.
- Lovejoy, S.: A voyage through scales, a missing quadrillion and why the climate is not what you expect, *Clim Dyn*, 44, 3187–3210, 2014.
- 290 Malamud, B. D. and Turcotte, D. L.: Self-affine time series: I. Generation and analyses, *Adv. Geophys*, 40, 1–90, 1999.
- WAIS Divide Project Members: Precise interpolar phasing of abrupt climate change during the last ice age, *Nature*, 520, 661–665, 2015.
- 295 Moberg, A., Sonechkin, D. M., Holmgren, K., Datsenko, N. M., and Karlén, W.: Highly variable Northern Hemisphere temperatures reconstructed from low- and high-resolution proxy data, *Nature*, 433, 613–617, 2005.
- Morice, C. P., Kennedy, J. J., Rayner, N. A., and Jones, P. D.: Quantifying uncertainties in global and regional temperature change using an ensemble of observational estimates: The HadCRUT4 data set, *J. Geophys. Res.*, 117, D08101, 2012.
- 300 Rypdal, K., Rypdal, M., and Fredriksen, H.-B.: Spatiotemporal Long-Range Persistence in Earth’s Temperature Field: Analysis of Stochastic-Diffusive Energy Balance Models, *J. Climate*, 28, 8379–8395, 2015.

Rypdal, M. and Rypdal, K.: Long-Memory Effects in Linear Response Models of Earth's Temperature and Implications for Future Global Warming, *J. Climate*, 27, 5240–5258, 2014.

305 Rypdal, M. and Rypdal, K.: Is there long-range memory in solar activity on timescales shorter than the sunspot period?, *J. Geophys. Res.*, 117, A04103, 2012.

Svensson, A., Andersen, K. K., Bigler, M., Clausen, H. B., Dahl-Jensen, D., Davies, S. M., Johnsen, S. J., Muscheler, R., Parrenin, F., Rasmussen, S. O., Röthlisberger, R., Seierstad, I., Steffensen, J. P., and Vinther, B. M.: A 60 000 year Greenland stratigraphic ice core chronology, *Clim. Past*, 4, 47–57, 2008.

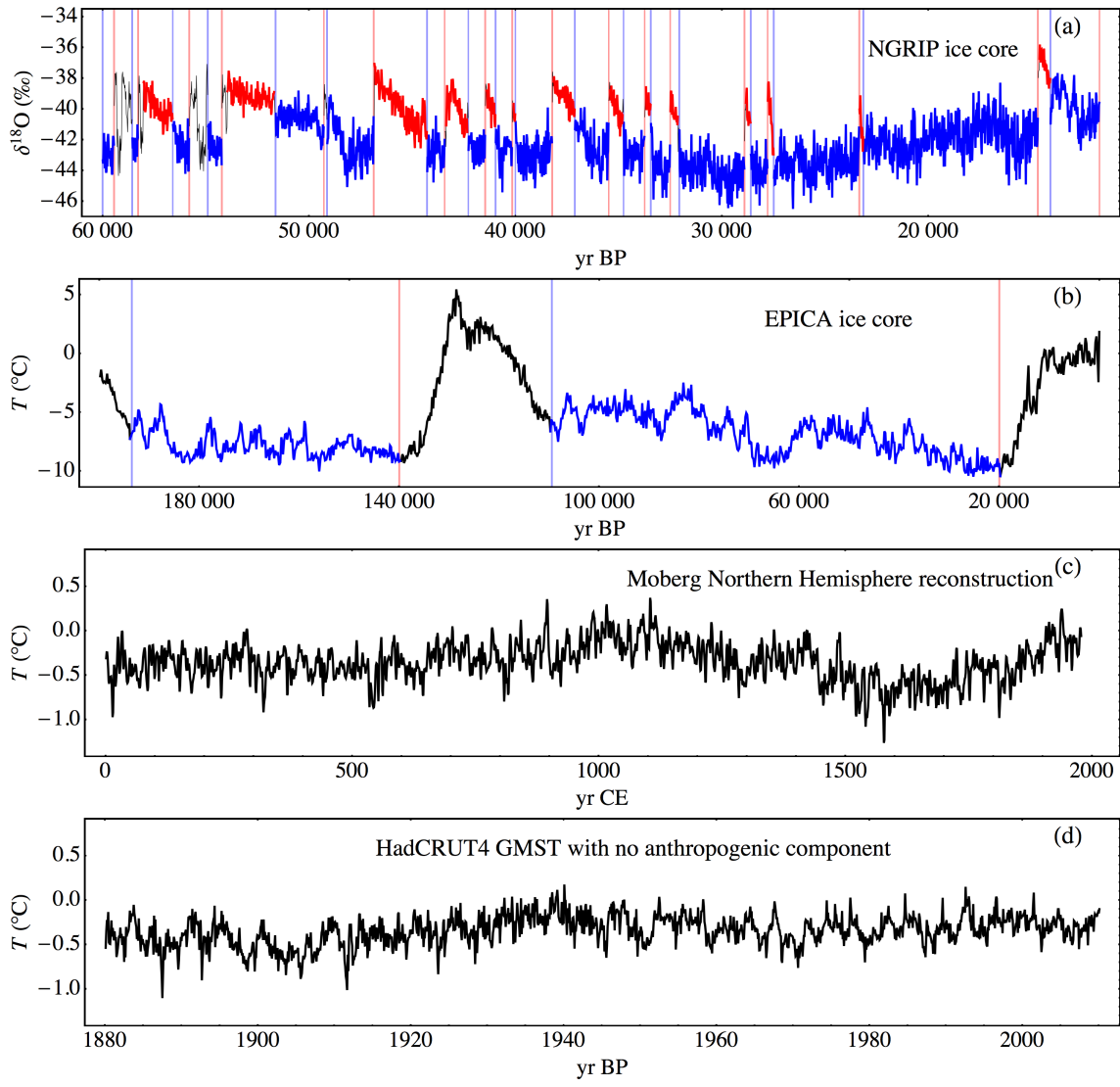


Figure 1. (a): The $\delta^{18}\text{O}$ concentration in the NGRIP ice core dating back to 60 kyr before present (BP). Here present means AD 2000 (= 2000 CE). The data is given as 20-year mean values. The time series is split into stadial (blue) and interstadial (red) periods. (b): The temperature reconstruction from the EPICA ice core. The shown time series is sampled with a time resolution of roughly 200 years. The temperature curve in the glacial periods is given in a blue color. (c): The Moberg reconstruction for the mean surface temperature in the Northern Hemisphere. The data is given with annual resolution. (d): The HadCRUT4 monthly global mean surface temperature where the anthropogenic component has been removed using a linear-response model.

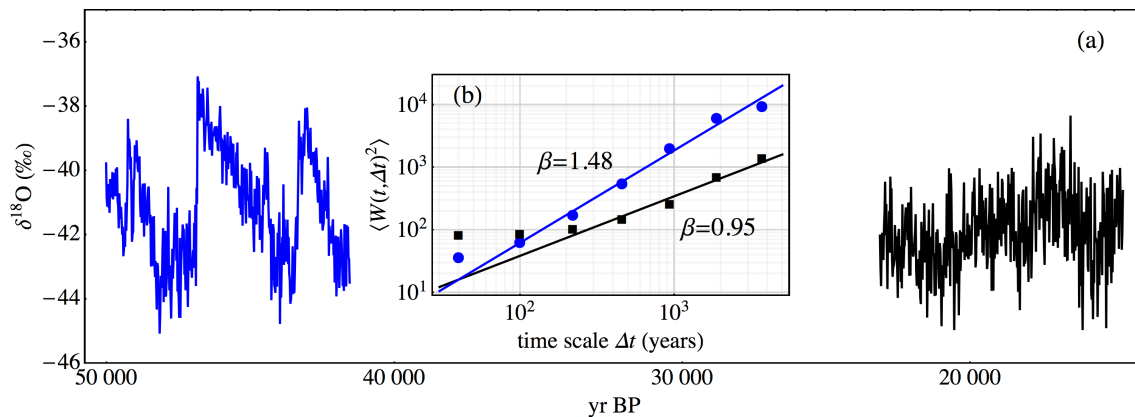


Figure 2. (a): The $\delta^{18}\text{O}$ concentration in the NGRIP ice core. The data is given as 20-yr mean values. Two different parts of the the times series is shown. The blue curve represents the $\delta^{18}\text{O}$ concentration in a time period starting approximately 50 kyr before present (BP) and has a duration of approximately 8500 years. As in Fig. 1, present means AD 2000 (= 2000 CE). The black curve represents the $\delta^{18}\text{O}$ concentration in a long stadial period that started about 22 kyrs BP and has a duration of approximately 8500 years. (b): The wavelet scaling functions estimated from the two parts of the NGRIP data set. The blue points are the estimates from the part of the NGRIP ice core that is shown as a blue curve in (a), and which contains DO cycles. The black points are the estimates from the the part of the NGRIP ice core that is shown as a black curve in (a), and which does not contain any DO cycles.

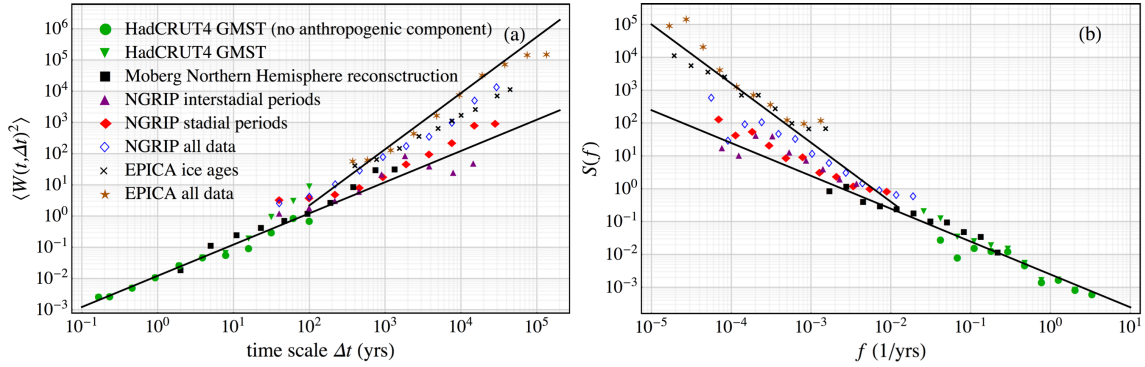


Figure 3. (a): For each time series considered in this paper we show double-logarithmic plots of the wavelet fluctuation $\langle |W(t, \Delta t)|^2 \rangle$ as a function of the time scale Δt . The green triangles and the green circles represent the the HadCRUT4 monthly global mean surface temperatures with and without the anthropogenic component respectively. The black circles is the analysis of the Moberg Northern Hemisphere reconstruction. The analysis of the 20-yr mean NGRIP data is shown as the blue diamonds, the purple triangles and the red diamonds. The blue diamonds show the results of the analysis of the entire dataset dating back to 60 kyrs BP. The red diamonds are the results of the analysis performed on the stadial periods only, and the purple triangles are the results of the analysis of the interstadial periods only. The results for the EPICA ice core data are shown as the orange stars and the black crosses. The orange stars are obtained by analysis of the entire data set dating back 200 kyrs, and the black crosses are obtained by only analysing the two most recent glaciations. The two solid lines have slopes $\beta = 1$ and $\beta = 1.8$. (b): As in (a), but instead of the wavelet fluctuation function we show the spectral density function $S(f)$. The two solid lines have slopes $-\beta$ with $\beta = 1$ and $\beta = 1.8$.

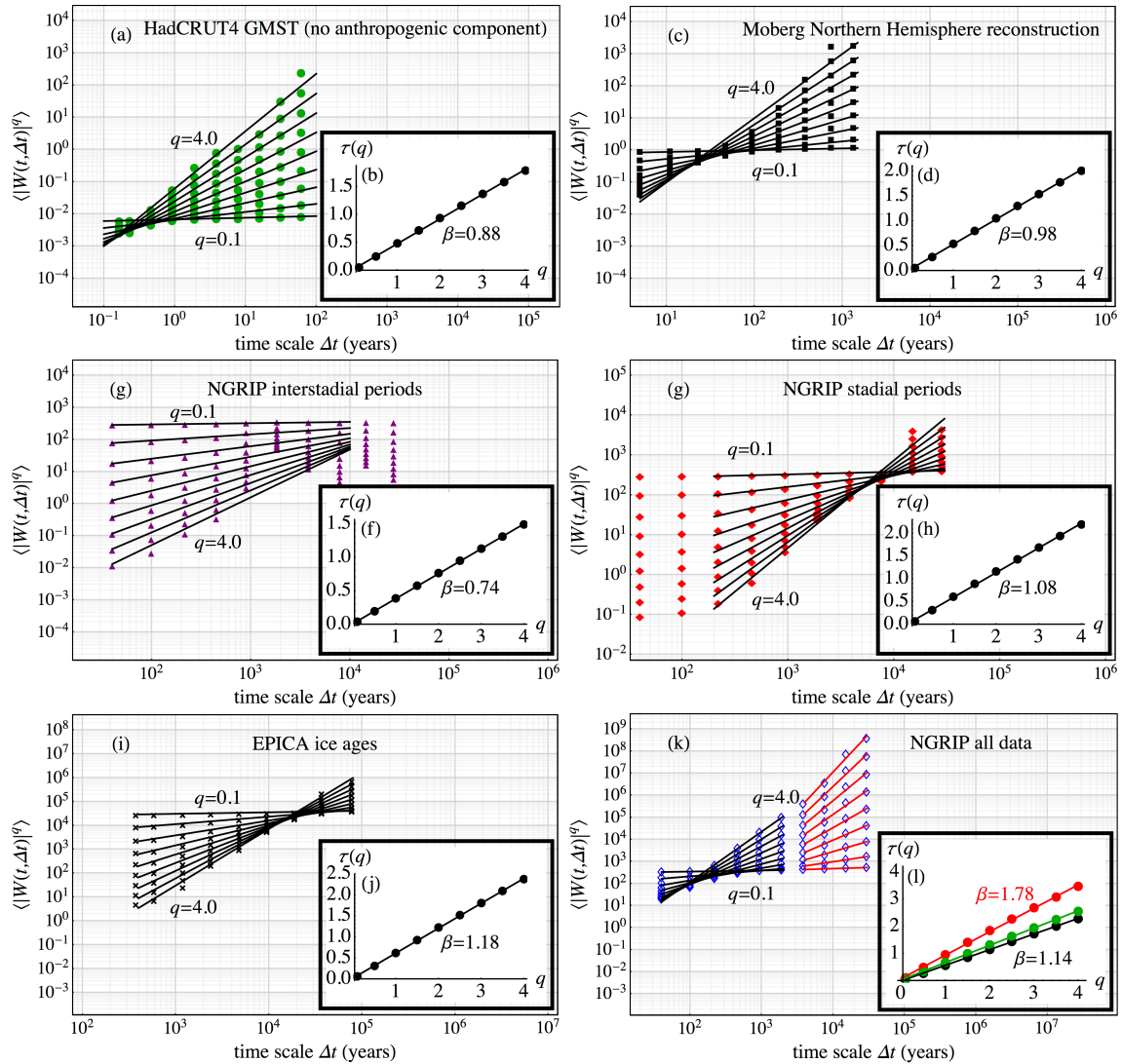


Figure 4. (a): The estimated wavelet-based structure functions $\langle |W(t, \Delta t)|^q \rangle$ for the HadCRUT4 monthly global mean surface temperature where the anthropogenic component has been removed using a linear-response model. The lines show the fitted power-law functions $c_q \Delta t^{\tau(q)}$. The q -values are $q = 0.1, 1.0, 1.5, \dots, 4.0$. (b) The scaling function $\tau(q)$ obtained from the fitted power-laws in (a). The line is a linear fit to the estimated scaling function, and the slope of this line is $\beta/2$ with $\beta = 0.88$. (c-d): As (a) and (b) but in this case for the Moberg Northern Hemisphere reconstruction. (g-f):